IEEE Access
Multidisciplinary | Rapid Review | Open Access Journal

Received November 23, 2020, accepted December 10, 2020, date of publication December 14, 2020,
date of current version December 30, 2020.

Digital Object Identifier 10.1109/ACCESS.2020.3044522

Electromechanically Deployable High-Gain Pop-Up Antenna Using Shape Memory Alloy and Kirigami Technology

SYED IMRAN HUSSAIN SHAH, (Member, IEEE), ANIRBAN SARKAR, (Member, IEEE), AND SUNGJOON LIM, (Member, IEEE)
School of Electrical and Electronic Engineering, Chung-Ang University, Seoul 156-756, South Korea

Corresponding author: Sungjoon Lim (sungjoon@cau.ac.kr)

This work was supported by the National Research Foundation of Korea (NRF) grant funded by the Korean Government (MSIT) under Grant 2017R1A2B3003856 and Grant 2018R1A4A1023826.

ABSTRACT This article proposes a low-cost, high-gain, and vertically polarized deployable antenna utilizing kirigami pop-up geometry. It primarily utilizes a foldable polyethylene terephthalate sheet to produce kirigami geometry in association with a rectangular radiating monopole, two reflectors, and a parasitic strip director. The reflectors and director increase the antenna gain and provide a frequency-independent tilted radiated beam with a higher beamwidth in the azimuth plane. In addition, electromechanically excited shape memory alloy (SMA) actuators enable folding and unfolding, make the antenna easily transportable and swiftly deployable. We describe the step-by-step fabrication of the kirigami geometry and shape memory spring actuator characterization. The designed, fabricated, and tested antenna achieves a −10 dB reflection bandwidth of 48.8% (1.7–2.8 GHz) providing a peak gain of more than 10 dBi at 2.45 GHz. The tilted radiated beam has a significantly wider beamwidth (90°) in the azimuth plane, compared to 40° in the elevation plane. The measured results agree well with simulations, verifying the proposed design concept. The fabricated prototype offers cost-effectiveness, more rapid fabrication, unprecedented performance, and significant potential for use in a range of microwave applications.

INDEX TERMS Deployable antenna, kirigami technology, shape memory alloy actuator, high-gain antenna.

I. INTRODUCTION

The rapid growth in military communication systems has led to the demand for new standards of deployable antennas with high gain, a tilted beam, and a wide beamwidth. Lightweight, high-gain, and deployable antennas that operate in the microwave frequency range are particularly suited for military communication because conventional satellite antennas are quite bulky, requiring vehicular or helicopter transport [1]. In general, a tilted-beam antenna with high-gain characteristics can be created by fabricating an array of multiple radiating elements and electronically adjusting their phase at the input ports [2]–[7].

A number of directive high-gain antennas with tilted beams based on different technologies have been reported [5], [8]–[10], but lightweight, high-gain origami/kirigami antennas represent a particularly attractive option because these folded antennas can easily be carried by military personnel and subsequently unfolded and deployed in the desired location [1].

Origami, which was first developed in Japan, involves the design of various crafts based on the folding and unfolding of paper sheets. Origami concepts have recently been employed in various interesting applications, including mechanical metamaterials [11], flexible electronics [12], soft folding robots [13], pneumatic actuators [14] and several others [15]–[17]. It offers a number of advantages, such as a lightweight design, easier deployment, and easier and faster fabrication. The benefits of origami in practical applications have recently been demonstrated with the fabrication of high-gain antennas. For example, a high-gain, tilted-beam, deployable origami antenna [18] using tetrahedron geometry achieved a gain of more than 9 dBi with a 60° tilted beam. However, the direction of the main beam changed at different frequencies due to the lossy paper substrate, and transportation was challenging due to the bulky dimensions

The associate editor coordinating the review of this manuscript and approving it for publication was Masood Ur-Rehman.

of the antenna. A high-gain deployable antenna using origami magic spiral cubes achieved a peak gain of 7.3 dBi, but fabrication was time consuming due to the construction including 3 magic cubes [19]. Another deployable origami antenna [1], [20] was designed for military applications, with a 60° tilted main beam. However, a gain of only 5.7 dBi was achieved with a significant side lobe level (1 dB) and a narrow beamwidth (60°). In addition, an origami-inspired deployable 2×2 corporate-fed microstrip patch antenna array [21] that could be easily reconfigured using a Miura-ori fold pattern was fabricated and achieved a gain of 5 dBi. Despite these advances, some earlier origami antennas suffered from low efficiency, limited flexibility, and spatial complexity. For example, the origami antennas reported in [1], [18], [20], were intended to be carried as paper sheets and fabricated when needed; however, fabrication was time-consuming and the final antennas were not robust.

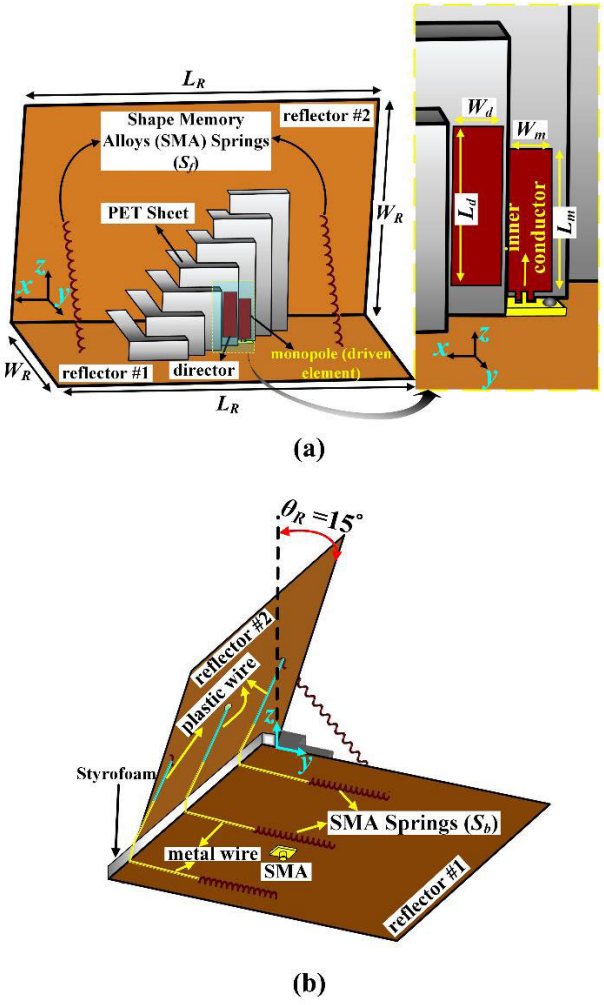

FIGURE 1. Proposed electromechanically deployable high-gain pop-up antenna geometry using a shape memory alloy and kirigami technology: (a) front view where $L_r = 250$ mm, $W_r = 200$ mm, $L_m = 30$ mm, $W_m = 10$ mm, $L_d = 30$ mm, and $W_d = 10$ mm, and (b) rear view.

Kirigami is an alternative form of origami that includes paper cutting and represents a notable advancement in origami technology. It retains all of the original benefits of the origami technology and incorporates additional features, including a greater degree of freedom in terms of flexibility and the final shape. Origami is mainly based on folding and unfolding techniques, whereas kirigami geometries are constructed by making cuts in the planar substrate sheets before folding. Consequently, the sheets can be transformed into complex three-dimensional (3D) patterns producing compression and tension [22]–[28]. A desired shape can be realized by making positional-dependent cuts in specific patterns on a flexible substrate to enhance reconfigurability via stretching, twisting, and bending. Thus, kirigami technology has been extended from paper substrates to the use of more robust and/or flexible substrates. This approach has recently received significant attention because of its use in deployable, foldable, stretchable, transformable, and reconfigurable electronics [26], [27]. For example, several studies have demonstrated lithium-ion batteries and supercapacitors fabricated using kirigami technology [23], [24], [27], and it has also been useful for the development of biomedical strain sensors [28]. Kirigami also opens new avenues for antenna design due to its various advantages, including its cost-effectiveness, lightweight nature, flexibility, convenient transportation, and rapid deployment. It not only has lower fabrication costs and a more rapid manufacturing process but can also be exploited for antenna geometries that are prohibitively difficult to achieve using conventional approaches [15]–[17].

In addition, to enhance the coverage range and field of view of tilted antennas, a wide beamwidth in the azimuth plane and a narrower beamwidth in the elevation plane are required. Because most users are close to the ground, power transmitted into the sky is wasted and should be reduced where possible [29]. However, most current tilted-beam, high-gain antennas suffer from a limited tilted bandwidth or a narrow beamwidth.

This article reports a high-gain antenna with a wide beamwidth in the azimuth plane. Compared with conventional high-gain antennas, the proposed antenna is vertically polarized, which is less prone to path loss and hence more likely to achieve superior radiation performance and offers stronger security [30]–[33]. The vertical monopole configuration is realized by exploiting kirigami pop-up geometry. We employ a foldable polyethylene terephthalate (PET) sheet to form the kirigami geometry in association with a rectangular radiating monopole, two printed-circuit-board (PCB) reflectors, and a parasitic strip director. The reflectors and director increase the antenna gain and provide a frequency-independent tilted radiated beam with a higher beamwidth in the azimuth plane. The inclusion of shape memory alloy (SMA) actuators allow the antenna to be folded and unfolded, making it easily transportable and swiftly deployable. We optimize the kirigami fabrication process and the characteristics of the SMA spring actuators in designing the proposed prototype. The fabricated prototype offers cost-effectiveness, more rapid fabrication, and unprecedented performance. It also exhibits significant potential for use in

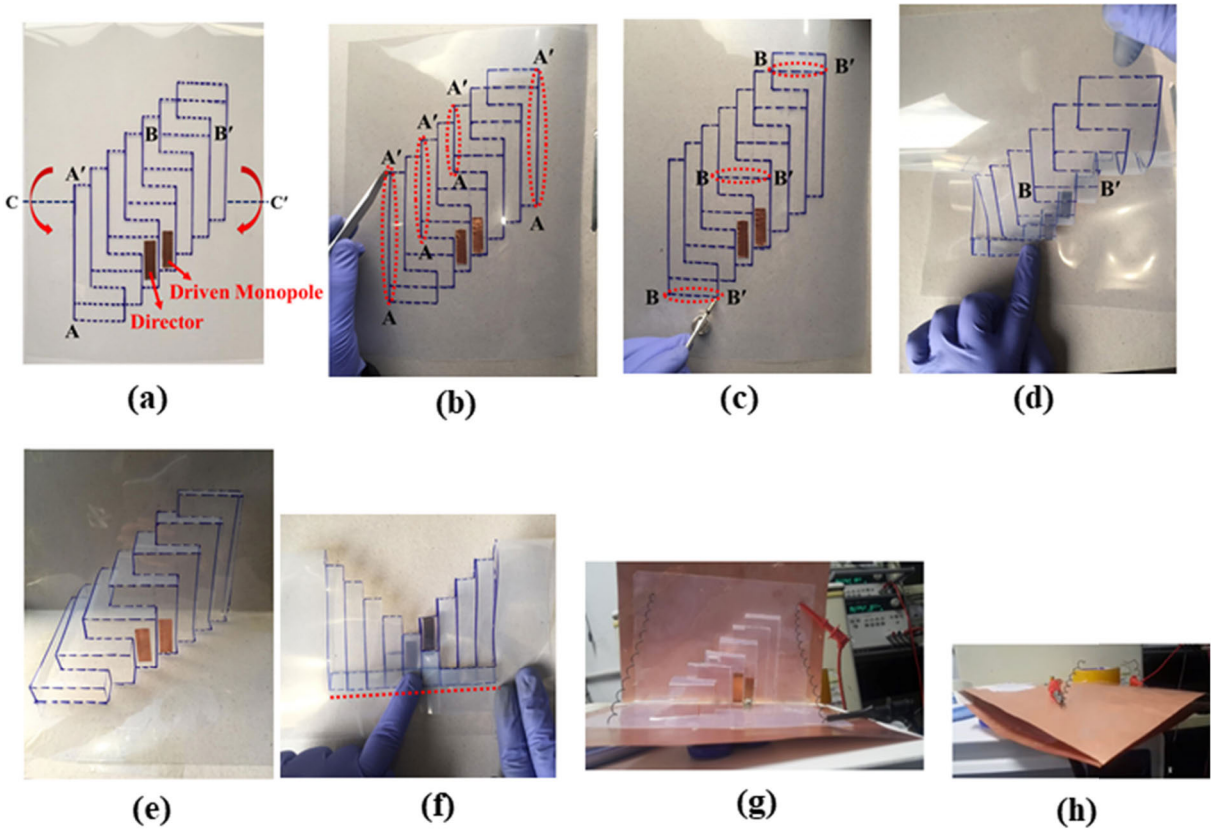

FIGURE 2. Fabrication steps for the kirigami antenna: (a) PET sheet with a printed pattern and attached copper film, (b) cut vertical lines, (c) etched horizontal lines, (d) folds along the horizontal lines to form a staircase geometry, (e) front view of the fabricated kirigami geometry, (f) final proposed kirigami geometry in its folded state (g) the antenna in unfolded form, and (h) folded state.

microwave applications related to military communication for tanks.

The remainder of this article is organized as follows. Section II describes the design principles of the kirigami antenna, including the overall fabrication process and rigorous parametric analysis. Section III discusses the electromechanical actuator and its application in the proposed antenna for folding and unfolding. Section IV presents a detailed design analysis and validation of the proposed antenna by comparing simulation and experimental results. Finally, a conclusion is drawn in section V, discussing the advantages and limitations of the proposed antenna.

II. KIRIGAMI ANTENNA SYSTEM

A. KIRIGAMI ANTENNA DESIGN

The proposed antenna comprises a rectangular monopole as the driven element with two reflectors and a director. We utilize kirigami geometry to design the antenna, with hard copper PCB sheets as the reflector elements. The pop-up geometry based on folding and unfolding ensures that the antenna is readily deployable. Figure 2 shows the individual design steps for the proposed kirigami geometry.

We use a PET sheet (145 mm × 145 mm, 0.25 mm thick) for physical robustness. The kirigami pattern is then printed onto the PET substrate, as shown in Fig. 2(a). Two copper strips (0.1 mm thick) are attached to the PET sheet, one serving as the driven monopole and the other as the director. The optimized monopole and director dimensions are 30 mm × 10 mm, with the director positioned 6 mm above the driven monopole.

To achieve the desired kirigami geometry, the PET sheet is segmented into various horizontal dashed lines (labelled BB') and vertical solid lines (labelled AA'). The PET sheet is then folded and unfolded along CC', dividing it into two sections. All of the vertical solid lines are cut with a standard cutter (Fig. 2b) and the horizontal lines etched sharply with compass (Fig. 2c).

All of the horizontal segments are sequentially folded starting from lower horizontal segments (Fig. 2d), and the unfolded kirigami design produces a 3D staircase shape (Fig. 2e). The kirigami geometry consists of seven steps, with the driven monopole on the third and the director on the fourth step; hence, the director is 6 mm higher than the driven monopole (Fig. 2a). The Kirigami structure allows it to be folded and unfolded; Fig. 2(f) shows it in its folded state. Two copper PCB sheets are attached to the back of the kirigami geometry to act as reflectors and support for the antenna to ensure it is sufficiently robust. Folding and unfolding

are realized using SMA springs that can be expanded and compressed/squeezed under the user's control to provide electronic tunability. Figs. 2(g) and (h) show the assembled antenna in its unfolded (i.e., operational) and folded states, respectively. The SMA actuators attached to the back of the geometry allow reflector #2 to be unfolded to 15° from the Z-axis. The antenna is excited using a 50-Ω subminiature version A connector with the inner pin connected to the rectangular monopole (Fig. 1) and the ground connected to the reflector.

We perform full-wave simulation for the proposed antenna using the ANSYS High-Frequency Structure Simulator (HFSS), with a dielectric constant and dielectric loss tan δ of 3 and 0.02, respectively for the PET sheet [34], and a copper film conductivity of 4.4×10^5 S/m [19]. Although this is lower than typical copper conductivity (5.96×10^7 S/m) [35], it is sufficient to ensure reasonable efficiency [16].

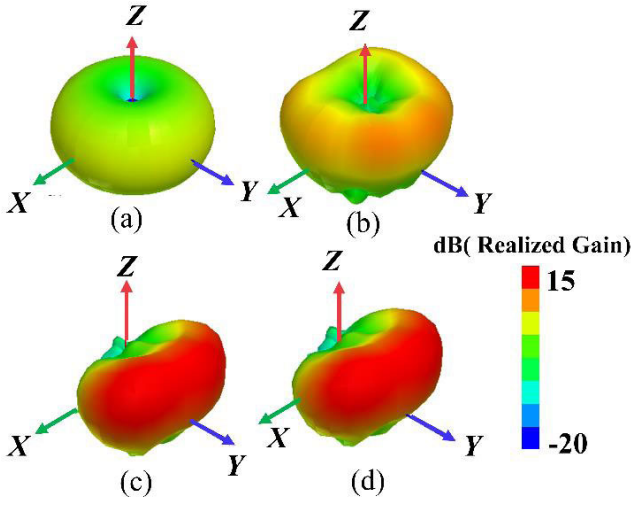

FIGURE 3. Radiation patterns for the proposed antenna steps: (a) monopole without reflectors or director, (b) only reflector #1, (c) reflectors #1 and #2, and (d) reflectors and director.

B. ANTENNA ELEMENT EFFECTS ON THE RADIATION PATTERNS

Several antenna element combinations are considered to realize the desired tilted radiation pattern and beamwidth. Fig. 3(a) shows the simulated 3D radiation pattern for a monopole antenna without a reflector or director. The antenna exhibits an omnidirectional pattern with a gain of only −0.1 dBi. We include reflector #1 to provide directionality and to increase the gain.

Figure 3(b) shows the corresponding simulated 3D radiation pattern with a gain of 4.5 dBi. Reflector #2 is then added to provide a 60° tilted radiation pattern (Fig. 3c), subsequently enhancing the gain to 9.6 dBi. Finally, we place a 14-mm long rectangular strip director from the driven element to increase the gain in the direction of the tilted beam. The final antenna design achieves a peak gain of 10.55 dBi with a tilted beam direction of 60° in the elevation plane (Fig. 3d).

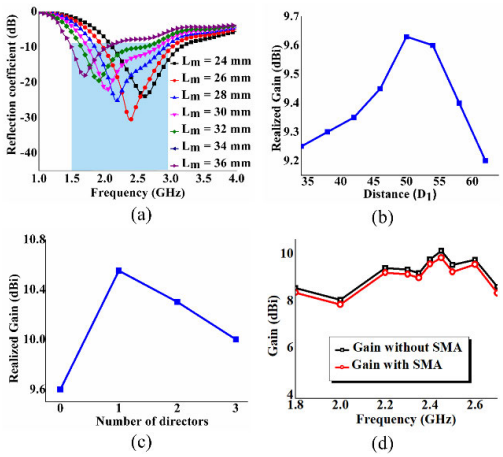

FIGURE 4. Parametric analysis of the proposed antenna: (a) resonance frequency with respect to monopole length, (b) gain with respect to the distance between the reflector and monopole, (c) gain with respect to the number of directors, and (d) gain with or without SMAs.

C. PARAMETRIC ANALYSIS

We conduct parametric analysis to study the effect of the design parameters on the antenna properties. In particular, we consider the monopole length (L_m), the distance between the rectangular monopole and reflector #2 (D_1), and the number of parasitic directors in seeking to optimize the resonance frequency with a suitable peak gain and beamwidth. Fig. 4(a) shows a decrease in frequency with increasing L_m. Because the desired resonance frequency is 2.4 GHz, we select L_m = 26 mm. The effect of D_1 on the antenna peak gain without any director can be observed in Fig. 4(b), where the peak gain increases to 9.6 dBi by increasing D_1 to 50 mm and subsequently decreases. Therefore, we select $D_1 = 50$ mm to achieve the highest peak gain with reflector #2. Figure 4(c) shows the simulated peak gain with respect to the number of directors. A single director increases the gain to 10.60 dBi from 9.60 dBi, but a second director reduces it to 9.58 dBi.

The proposed antenna geometry produced a wider beamwidth than conventional Yagi antennas, hence adding a second director did not increase the antenna gain. Therefore, we used a single director, achieving a peak gain of more than 10 dBi with a large beamwidth in the azimuth plane. We use SMA actuators to electronically fold and unfold the antenna geometry. Figure 4(d) compares the gain achieved with respect to the operating frequency with and without the SMA actuators. The actuators have a negligible effect on antenna performance because their length is much longer than the monopole antenna. Although reflector #2 can only be unfolded to 15°, simulations verify that this has no effect on the characteristics of antenna performance, including impedance matching, peak gain, and elevation beam direction.

III. EXPERIMENTAL VERIFICATION OF THE ELECTROMECHANICAL ACTUATORS

A. ELECTROMECHANICAL ACTUATORS

SMA springs are electromechanical actuators that can be deformed depending on the applied excitation voltage.

The SMA actuators employed to fold and deploy the proposed kirigami geometry have a thin contraction-type helical structure with a strong temperature-dependent linear actuation without the need for moving parts. Applying a suitable voltage for a given period will restore the SMA shape and retain it until it is mechanically deformed at room temperature. This way, even though the spring is elongated at room temperature by applying an external force, passing DC through it will restore its original length. The selected SMA spring can be extended to approximately 130 mm at room temperature, and it possesses a force of 5 N during contraction. This pulling force is imposed to fold and unfold the proposed antenna geometry by increasing the total spring length to more than 80% of the initial compressed state.

Because an SMA spring has one-way memory, the proposed geometry employ springs on the front face (S_f) to fold the antenna geometry, and three springs are employed on the back (S_b) to unfold it. Therefore, this set of actuators is responsible for the folding and deployment of the antenna. The folded and unfolded state of reflector #2 (see Fig. 1) reflects the corresponding folding and deployment of the kirigami geometry, keeping reflector #1 stationary. In particular, applying approximately 2 V to S_f compresses the springs to fold reflector #2, and elongate S_b. Similarly, passing current through S_b unfolds the kirigami geometry.

SMA spring actuators with an extended length of 130 mm are required to fold and unfold the geometry. The selected SMA springs require 23 seconds to contract and are relatively insensitive to minor fluctuations in ambient temperature. SMA springs have been previously used in the design of frequency- and pattern-reconfigurable antennas [37], [38]. It is important to note that SMA-based switching cannot compete with other tunable and switchable microwave devices in terms of speed. This slow response speed is attributed to inefficient heat transfer [39]. Recently, research on SMA actuators has increased substantially, particularly in terms of their actuation speed, which can be enhanced with quick heating. For example, a fast and energy-efficient actuation strategy has been proposed based on short pulses in the millisecond range to reduce actuation times to approximately 20 ms [39], [40]. This approach can also reduce the energy used by up to 80% compared with conventional quasi-static actuation. Therefore, we expect that the low-switching speed of SMA actuators will be solved in the near future.

B. SHAPE MEMORY ALLOY ACTUATOR CHARACTERIZATION

In the spring characterization process, external DC excitation voltage ranging from 0.7 V to 2 V with a current of 3 A is applied to the open ends of the SMA springs (Fig. 5a). This provides a clear indication of the limits of their stretching ability. We define stretching as the total variation in the spring length divided by the time elapsed. Initial stretching is approximately 180 mm/s for a pitch of 9 mm, which is considered the fully stretched state. Figure 5(b) shows that, with the application of 2.58 W, the spring starts compressing

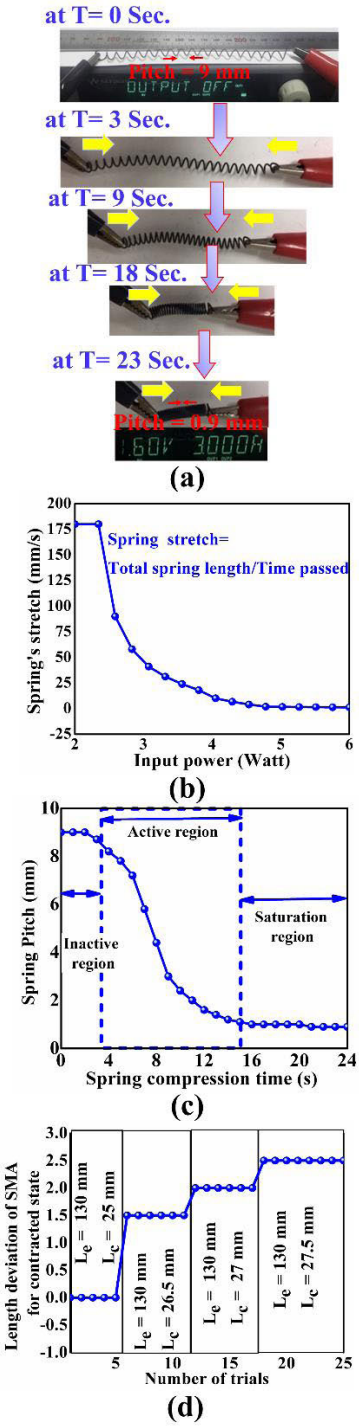

FIGURE 5. Shape memory alloy (SMA) actuator spring characterization: (a) compression and squeezing analysis, (b), (c) spring pitch against spring compression time, and (d) repeatability analysis of the maximum deviation in length of the compressed state.

and continues until 4.5 W, at which the stretching is only 4 mm/sec, negligible actuation is observed beyond this. Figure 5(c) presents the active spring region with respect to time. The spring acts very quickly for approximately 10 s. Actuation starts after 3 s and the spring pitch decreases until 15 s. The spring demonstrates almost no subsequent actuation

with an input power of 4.5 W. Figure 5(d) displays the results of the test for SMA spring repeatability, in which the selected SMA spring is compressed multiple times from its fully expanded state ($L_e = 130$ mm) using the applied voltage.

A maximum deviation of 2.5 mm is observed from the initial compressed state ($L_c = 25$ mm) after 25 trials, which alters the tilted beam angle of the proposed antenna by only 2°. Hence, the proposed SMA-based beam-reconfigurable antenna shows acceptably stable performance after repeated use.

IV. EXPERIMENTAL VERIFICATION OF ANTENNA PERFORMANCE

The proposed deployable kirigami antenna is fabricated on a PET sheet (Fig. 2). The S-parameter of the antenna is measured using an Anritsu MS2038C vector network analyzer, and a comparison of the simulated and measured reflection coefficients are presented in Fig. 6. The simulated and measured reflection coefficients are in good agreement, covering a frequency range of 1.7–2.8 GHz, with a −10 dB impedance bandwidth of 48.8%.

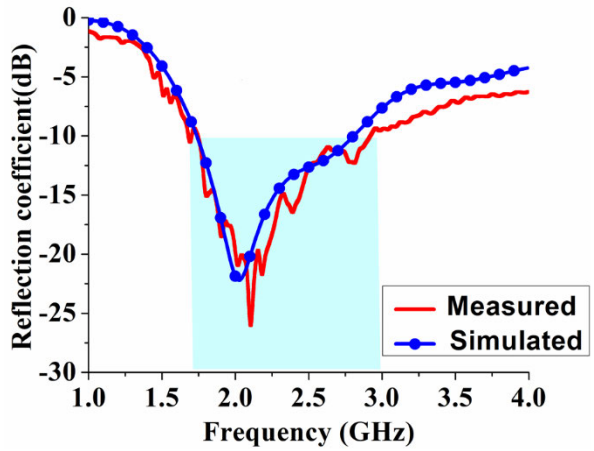

FIGURE 6. Simulated and measured reflection coefficients for the proposed deployable kirigami antenna.

The minor difference between the simulated and measured reflection coefficients is due to folding errors and fabrication tolerance. The 3D radiation pattern of the antenna is measured in a shielded commercial radio frequency anechoic chamber. The simulated and measured 2D radiation patterns of the antenna in the elevation plane are presented for frequencies of 1.8, 2.1, and 2.4 GHz in Fig. 7.

The main beam of the antenna is directed towards θ of 60° for all frequencies. The two reflectors and the director are employed to achieve the desired tilted beam. Figure 8 shows that the measured normalized radiation patterns in the azimuth plane achieve a beamwidth of more than 90°. The combination of the two reflectors and the director also helps to achieve a wide beamwidth in the azimuth plane. The measured 3D radiation patterns for the antenna at frequencies of 1.8, 2.1, and 2.4 GHz are depicted in Fig. 9.

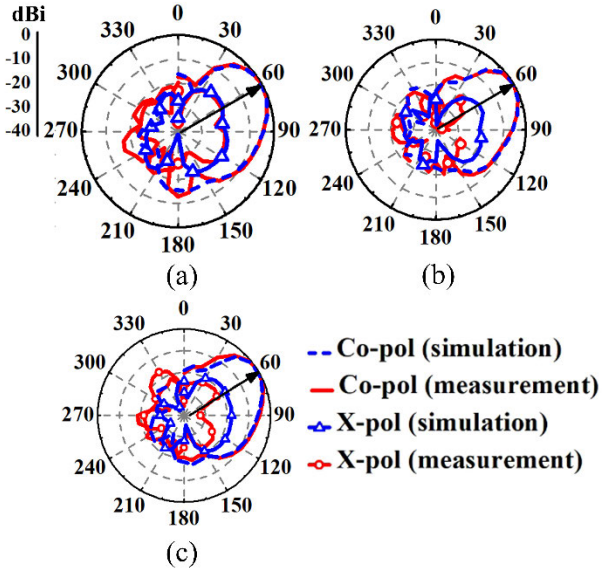

FIGURE 7. Simulated and measured normalized radiation patterns in the elevation plane at (a) 1.8, (b) 2.1, and (c) 2.4 GHz.

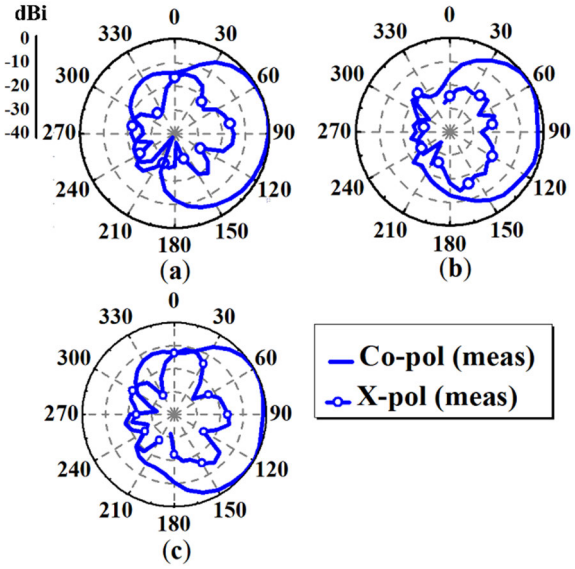

FIGURE 8. Measured normalized radiation patterns in the azimuth plane at (a) 1.8, (b) 2.1, and (c) 2.4 GHz.

In Fig. 10(a), the simulated and measured peak gains are plotted for the −10 dB impedance bandwidth of the antenna. At 2.4 GHz, the measured peak gain of the antenna is 10.3 dBi, compared to 10.6 dBi for the simulation. Figure 10(b) shows the simulated and measured radiation efficiency for the proposed antenna. The measured radiation efficiency is calculated from the ratio of the measured peak gain to the simulated directivity, achieving 76.47% to 96% over the antenna's entire operating impedance bandwidth.

This enhanced radiation efficiency is largely due to the low-loss PET sheet. As a result, the antenna efficiency is significantly higher than other previously reported paper-based

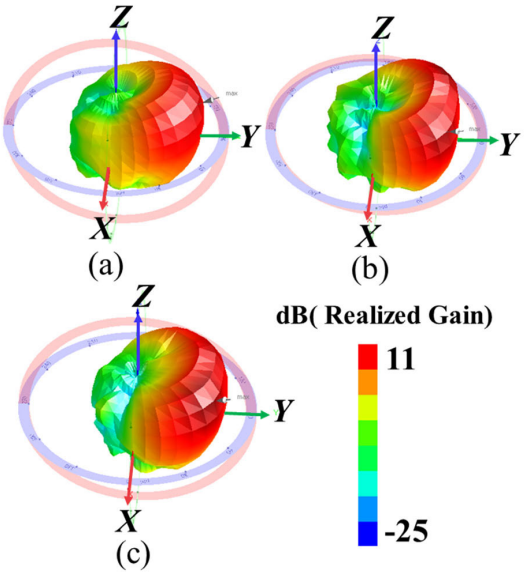

FIGURE 9. Measured 3D radiation patterns for the proposed antenna at (a) 1.8, (b) 2.1, and (c) 2.4 GHz.

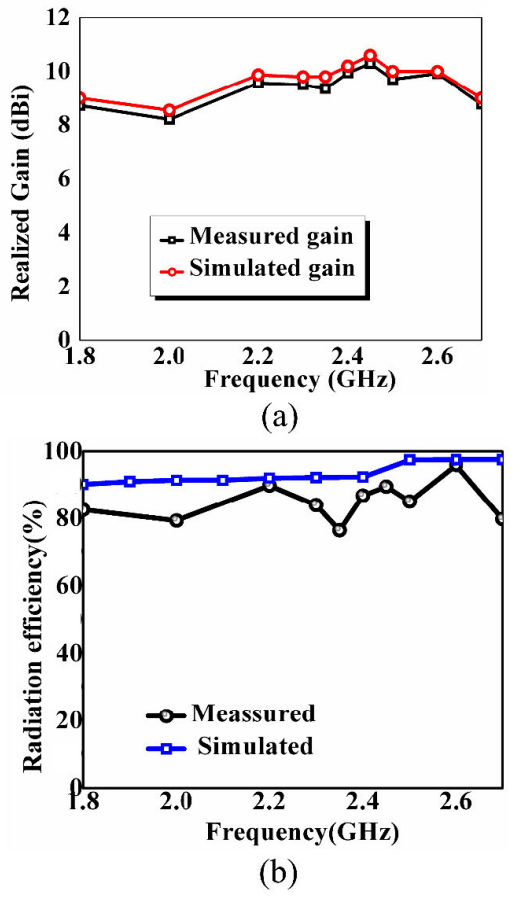

FIGURE 10. Simulated and measured (a) gain and (b) efficiency for the proposed deployable antenna.

origami antennas [18], [20], [41]. The proposed antenna also achieves a large beamwidth in the azimuth plane and offers swift mechanical deployment. In addition, the manufacturing

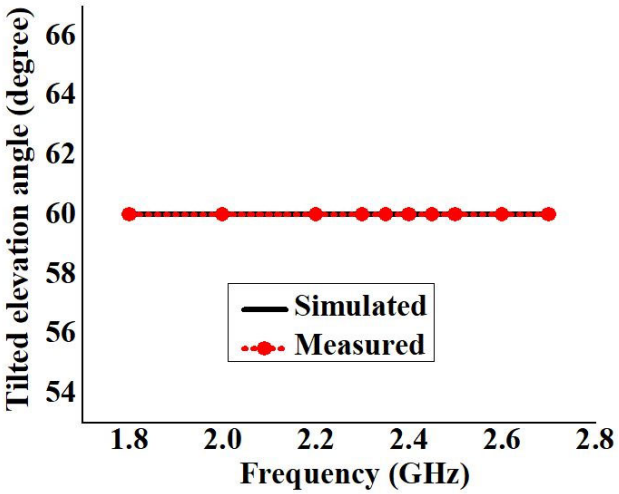

FIGURE 11. Simulated and measured beam direction for the proposed deployable antenna.

process is much simpler, faster, and easier than previously reported deployable antennas [18], [20], [41]. Compared to conventional high-gain antennas, the proposed antenna is vertically polarized, which reduces the path loss, and vertical wire antennas generally achieve better practical radiation performance and have greater security [30]–[33]. The proposed antenna is low-cost due to its simple and easily obtained parts.

V. CONCLUSION

This article presents a low-cost, lightweight, high-gain, vertically polarized deployable antenna based on a kirigami pop-up geometry. The antenna primarily utilizes a foldable PET sheet to form the kirigami geometry in association with a rectangular radiating monopole, two reflectors, and a parasitic strip director. Electromechanically excited SMA actuators allow the assembled antenna to be quickly stowed, ensuring easy transportability and swift deployment at the desired location.

The fabricated prototype achieves a −10 dB reflection bandwidth of 48.8% (1.7–2.8 GHz), a peak gain of more than 10 dBi at 2.45 GHz, and a 60° tilted radiated beam with significantly larger beamwidth (90°) in the azimuth plane.

The proposed antenna is suitable for tanks and other forms of military communication. Compared to existing conventional military field antennas, the proposed antenna is low-cost and offers very simple and rapid fabrication, making it suitable for numerous deployable antenna applications. Future deployable antennas can employ fast-switching SMA springs to further increase the deployment speed.

REFERENCES

[1] S. I. H. Shah, S. Lim, M. M. Tentzeris, S. Imran, H. Shah, and S. Lim, "Military field deployable antenna using origami," in *Proc. Int. Workshop Antenna Technol., Small Antennas, Innov. Struct., Appl. (iWAT)*, Oct. 2017, pp. 2–3, doi: 10.13140/RG.2.1.2023.8804.

[2] I. Kim and Y. Rahmat-Samii, "Beam-tilted dipole-EBG array antenna for future base station applications," in *Proc. IEEE Antennas Propag. Soc. Int. Symp. (APSURSI)*, Jul. 2013, pp. 1224–1225, doi: 10.1109/APS.2013.6711272.

[3] H. Nakano, S. Mitsui, and J. Yamauchi, "Tilted-beam high gain antenna system composed of a patch antenna and periodically arrayed loops," *IEEE Trans. Antennas Propag.*, vol. 62, no. 6, pp. 2917–2925, Jun. 2014, doi: 10.1109/TAP.2014.2311460.

[4] H. Nakano, Y. Asano, H. Mimaki, and J. Yamauchi, "Tilted beam formation by an array composed of strip inverted f antennas with a finite-sized EBG reflector," in *Proc. IEEE Int. Symp. Microw., Antenna, Propag. EMC Technol. Wireless Commun.*, Aug. 2005, pp. 438–441, doi: 10.1109/mape.2005.1617943.

[5] H. Nakano, M. Iwatsuki, M. Sakurai, and J. Yamauchi, "A cavity-backed rectangular aperture antenna with application to a tilted fan beam array antenna," *IEEE Trans. Antennas Propag.*, vol. 51, no. 4, pp. 712–718, Apr. 2003, doi: 10.1109/TAP.2003.811085.

[6] C. U. Lee, G. Noh, B. K. Ahn, J. W. Yu, and H. L. Lee, "Tilted-beam switched array antenna for UAV mounted radar applications with 360° coverage," *Electron.*, vol. 8, no. 11, pp. 1–11, 2019, doi: 10.3390/electronics8111240.

[7] G. Mansutti, F. Rigobello, S. M. Asif, M. S. Khan, A.-D. Capobianco, and A. Galtarossa, "Main lobe control of a beam tilting antenna array laid on a deformable surface," *Int. J. Antennas Propag.*, vol. 2018, pp. 1–6, Jan. 2018, doi: 10.1155/2018/2521953.

[8] A. Dadgarpour, B. Zarghooni, B. S. Virdee, and T. A. Denidni, "Beam tilting antenna using integrated metamaterial loading," *IEEE Trans. Antennas Propag.*, vol. 62, no. 5, pp. 2874–2879, May 2014, doi: 10.1109/TAP.2014.2308516.

[9] A. Dadgarpour, M. S. Sorkherizi, A. A. Kishk, and T. A. Denidni, "Single-element antenna loaded with artificial mu-near-zero structure for 60 GHz MIMO applications," *IEEE Trans. Antennas Propag.*, vol. 64, no. 12, pp. 5012–5019, Dec. 2016, doi: 10.1109/TAP.2016.2618485.

[10] W. Dale Ake, M. Pour, and A. Mehrabani, "Asymmetric half-bowtie antennas with tilted beam patterns," *IEEE Trans. Antennas Propag.*, vol. 67, no. 2, pp. 738–744, Feb. 2019, doi: 10.1109/TAP.2018.2880078.

[11] M. Eidini, "Zigzag-base folded sheet cellular mechanical metamaterials," *Extreme Mech. Lett.*, vol. 6, pp. 96–102, Mar. 2016, doi: 10.1016/j.eml.2015.12.006.

[12] Z. Song, T. Ma, R. Tang, Q. Cheng, X. Wang, D. Krishnaraju, R. Panat, C. K. Chan, H. Yu, and H. Jiang, "Origami lithium-ion batteries," *Nature Commun.*, vol. 5, no. 1, pp. 1–6, May 2014, doi: 10.1038/ncomms4140.

[13] J. Li, H. Godaba, Z. Q. Zhang, C. C. Foo, and J. Zhu, "A soft active origami robot," *Extreme Mech. Lett.*, vol. 24, pp. 30–37, Oct. 2018, doi: 10.1016/j.eml.2018.08.004.

[14] R. V. Martinez, C. R. Fish, X. Chen, and G. M. Whitesides, "Elastomeric origami: Programmable paper-elastomer composites as pneumatic actuators," *Adv. Funct. Mater.*, vol. 22, no. 7, pp. 1376–1384, Apr. 2012, doi: 10.1002/adfm.201102978.

[15] S. Lee, M. Lee, and S. Lim, "Frequency reconfigurable antenna actuated by three-storey tower kirigami," *Extreme Mech. Lett.*, vol. 39, Sep. 2020, Art. no. 100833, doi: 10.1016/j.eml.2020.100833.

[16] Z. Zhang, B. Luce, C. Ma, B. Xie, and N. Hu, "Programmable origami-inspired cellular architected building blocks for flow-regulating adaptive weir," *Extreme Mech. Lett.*, vol. 40, Oct. 2020, Art. no. 100974, doi: 10.1016/j.eml.2020.100974.

[17] S. Sadeghi and S. Li, "Dynamic folding of origami by exploiting asymmetric bi-stability," *Extreme Mech. Lett.*, vol. 40, Oct. 2020, Art. no. 100958, doi: 10.1016/j.eml.2020.100958.

[18] S. I. H. Shah, D. Lee, M. M. Tentzeris, and S. Lim, "A novel high-gain tetrahedron origami," *IEEE Antennas Wireless Propag. Lett.*, vol. 16, pp. 848–851, 2017, doi: 10.1109/LAWP.2016.2609898.

[19] S. I. H. Shah, M. M. Tentzeris, and S. Lim, "A deployable quasi-yagi monopole antenna using three origami magic spiral cubes," *IEEE Antennas Wireless Propag. Lett.*, vol. 18, no. 1, pp. 147–151, Jan. 2019, doi: 10.1109/LAWP.2018.2883380.

[20] S. I. H. Shah, M. M. Tentzeris, and S. Lim, "Low-cost circularly polarized origami antenna," *IEEE Antennas Wireless Propag. Lett.*, vol. 16, pp. 2026–2029, 2017, doi: 10.1109/LAWP.2017.2694138.

[21] S. R. Seiler, G. Bazzan, K. Fuchi, E. J. Alanyak, A. S. Gillman, G. W. Reich, P. R. Buskohl, S. Pallampati, D. Sessions, D. Grayson, and G. H. Huff, "Physical reconfiguration of an origami-inspired deployable microstrip patch antenna array," in *Proc. IEEE Int. Symp. Antennas Propag. USNC/URSI Nat. Radio Sci. Meeting*, Jul. 2017, pp. 2359–2360, doi: 10.1109/APUSNCURSINRSM.2017.8073222.

[22] R. M. Neville, J. Chen, X. Guo, F. Zhang, W. Wang, Y. Dobah, F. Scarpa, J. Leng, and H.-X. Peng, "A kirigami shape memory polymer honeycomb concept for deployment," *Smart Mater. Struct.*, vol. 26, no. 5, May 2017, Art. no. 05LT03, doi: 10.1088/1361-665X/aa6b6d.

[23] C. Jianguo, D. Xiaowei, and F. Jian, "Morphology analysis of a foldable kirigami structure based on miura origami," *Smart Mater. Struct.*, vol. 23, no. 9, Sep. 2014, Art. no. 094011, doi: 10.1088/0964-1726/23/9/094011.

[24] Z. Song, X. Wang, C. Lv, Y. An, M. Liang, T. Ma, D. He, Y.-J. Zheng, S.-Q. Huang, H. Yu, and H. Jiang, "Kirigami-based stretchable lithium-ion batteries," *Sci. Rep.*, vol. 5, no. 1, pp. 1–9, Sep. 2015, doi: 10.1038/srep10988.

[25] A. Lamoureux, K. Lee, M. Shlian, S. R. Forrest, and M. Shtein, "Dynamic kirigami structures for integrated solar tracking," *Nature Commun.*, vol. 6, no. 1, pp. 1–6, Nov. 2015, doi: 10.1038/ncomms9092.

[26] A. Salim, A. H. Naqvi, E. Park, A. D. Pham, and S. Lim, "Inkjet printed kirigami inspired split ring resonator for disposable, low cost strain sensor applications," *Smart Mater. Struct.*, vol. 29, no. 1, Jan. 2020, Art. no. 015016, doi: 10.1088/1361-665X/ab548b.

[27] R. Xu, A. Hung, A. Zverev, C. Shen, L. Irie, G. Ding, M. Whitmeyer, L. Ren, B. Griffin, J. Melcher, L. Zheng, X. Zang, and L. Lin, "A kirigami-inspired, extremely stretchable, high areal-coverage micro-supercapacitor patch," in *Proc. IEEE Micro Electro Mech. Syst. (MEMS)*, Jan. 2018, pp. 661–664, doi: 10.1109/MEMSYS.2018.8346641.

[28] A. Baldwin and E. Meng, "Kirigami strain sensors microfabricated from thin-film parylene c," *J. Microelectromech. Syst.*, vol. 27, no. 6, pp. 1082–1088, Dec. 2018, doi: 10.1109/JMEMS.2018.2869090.

[29] S. Chattopadhyay, J. Y. Siddiqui, and D. Guha, "Rectangular microstrip patch on a composite dielectric substrate for high-gainwide-beam radiation patterns," *IEEE Trans. Antennas Propag.*, vol. 57, no. 10, pp. 3324–3327, 2009, doi: 10.1109/TAP.2009.2029607.

[30] J. Oh and K. Sarabandi, "Low profile vertically polarized omnidirectional wideband antenna with capacitively coupled parasitic elements," *IEEE Trans. Antennas Propag.*, vol. 62, no. 2, pp. 977–982, Feb. 2014, doi: 10.1109/TAP.2013.2291891.

[31] K. Ghaemi and N. Behdad, "A low-profile, vertically polarized ultra-wideband antenna with monopole-like radiation characteristics," *IEEE Trans. Antennas Propag.*, vol. 63, no. 8, pp. 3699–3705, Aug. 2015, doi: 10.1109/TAP.2015.2430880.

[32] A. A. Omar and Z. Shen, "A compact and wideband vertically polarized monopole antenna," *IEEE Trans. Antennas Propag.*, vol. 67, no. 1, pp. 626–631, Jan. 2019, doi: 10.1109/TAP.2018.2874698.

[33] A. H. Naqvi, J.-H. Park, C.-W. Baek, and S. Lim, "Via-monopole based quasi yagi-uda antenna for W-Band applications using through glass silicon via (TGSV) technology," *IEEE Access*, vol. 8, pp. 9513–9519, 2020, doi: 10.1109/ACCESS.2020.2964709.

[34] A. T. Castro and S. K. Sharma, "Inkjet-printed wideband circularly polarized microstrip patch array antenna on a PET film flexible substrate material," *IEEE Antennas Wireless Propag. Lett.*, vol. 17, no. 1, pp. 176–179, Jan. 2018, doi: 10.1109/LAWP.2017.2779440.

[35] S. Shah and S. Lim, "A dual band frequency reconfigurable origami magic cube antenna for wireless sensor network applications," *Sensors*, vol. 17, no. 11, p. 2675, Nov. 2017, doi: 10.3390/s17112675.

[36] S. Imran, H. Shah, and S. Lim, "Novel deployable Quasi-Yagi monopole antenna using origami magic spiral cube," in *Proc. Int. Symp. Antennas Propag. (ISAP)*, Oct. 2018, pp. 1–2.

[37] S. Jalali Mazlouman, A. Mahanfar, C. Menon, and R. G. Vaughan, "Reconfigurable axial-mode helix antennas using shape memory alloys," *IEEE Trans. Antennas Propag.*, vol. 59, no. 4, pp. 1070–1077, Apr. 2011, doi: 10.1109/TAP.2011.2109686.

[38] S. J. Mazlouman, A. Mahanfar, C. Menon, and R. G. Vaughan, "Square ring antenna with reconfigurable patch using shape memory alloy actuation," *IEEE Trans. Antennas Propag.*, vol. 60, no. 12, pp. 5627–5634, Dec. 2012, doi: 10.1109/TAP.2012.2213053.

[39] P. Motzki, T. Gorges, M. Kappel, M. Schmidt, G. Rizzello, and S. Seelecke, "High-speed and high-efficiency shape memory alloy actuation," *Smart Mater. Struct.*, vol. 27, no. 7, Jun. 2018, Art. no. 075047, doi: 10.1088/1361-665X/aac9e1.

[40] J. Qiu, J. Tani, D. Osanai, and Y. Urushiyama, "High-speed actuation of shape memory alloy," *Proc. SPIE*, vol. 4235, pp. 188–197, Mar. 2001, doi: 10.1117/12.420858.

[41] S. Shah and S. Lim, "Transformation from a single antenna to a series array using Push/Pull origami," *Sensors*, vol. 17, no. 9, p. 1968, Aug. 2017, doi: 10.3390/s17091968.

SYED IMRAN HUSSAIN SHAH (Member, IEEE) received the B.S. degree in telecommunication engineering and the M.S. degree in electrical engineering from the University of Engineering and Technology, Peshawar, Pakistan, in 2011 and 2014, respectively, and the Ph.D. degree from the School of Electrical and Electronics Engineering, Chung-Ang University, Seoul, South Korea, in 2020. He has authored more than 30 journals and conference articles focused on reconfigurable, deployable, and printed and smart antennas. His research interests include the design and the analysis of frequency and pattern reconfigurable origami antennas, deployable origami antennas, 3D printed antennas, and shape memory materials based smart antennas and implanted antennas.

ANIRBAN SARKAR (Member, IEEE) received the B.Tech. degree from the Department of Electronics and Communication Engineering, Hooghly Engineering and Technology College, India, in 2011, the M.E. degree in microwave communication from the Electronics and Telecommunication Engineering Department, Indian Institute of Engineering Science and Technology, Shibpur, India, in 2013, and the Ph.D. degree from the Department of Electrical Engineering in RF and microwave from IIT Kanpur, India, in 2019.

He joined as a Postdoctoral Fellow with the School of Electrical and Electronics Engineering, Chung-Ang University, Seoul, South Korea under the supervision of Prof. Sungjoon Lim. He has authored and coauthored more than 50 international conference, letter, and journal articles. His research interests include millimeter-wave leaky-wave antenna, and reconfigurable leaky-wave antennas. He served as a Reviewer for IEEE Access, the IEEE Transactions on Antennas and Propagation (TAP), *IET Electronics Letter*, *Microwave and Optical Technology Letters* (MOTL) (Wiley), *IET Microwave and Antenna Propagation*, Wiley, and RFCAD. He also served as a Secretary for the MTT-S Student Branch Chapter IIT Kanpur and Webmaster and as a Vice-Chair for the IEEE APS Student Branch Chapter IIT Kanpur.

SUNGJOON LIM (Member, IEEE) received the B.S. degree in electronic engineering from Yonsei University, Seoul, South Korea, in 2002, and the M.S. and Ph.D. degrees in electrical engineering from the University of California at Los Angeles (UCLA), Los Angeles, CA, USA, in 2004 and 2006, respectively.

After a postdoctoral position at the Integrated Nanosystem Research Facility (INRF), University of California at Irvine, Irvine, CA, USA, he joined the School of Electrical and Electronics Engineering, Chung-Ang University, Seoul, in 2007, where he is currently a Professor. He has authored and coauthored more than 250 international conference, letter, and journal articles. His research interests include engineered electromagnetic structures (metamaterials, electromagnetic bandgap materials, and frequency selective surfaces), printed antennas, substrate integrated waveguide (SIW) components, inkjet-printed electronics, and RF MEMS applications. He is also interested in the modeling and design of microwave circuits and systems.

Dr. Lim received the Institution of Engineering and Technology (IET) Premium Award, in 2009, the ETRI Journal Best Paper Award, in 2014, the Best Paper Award in the 2015 International Workshop on Antenna Technology (iWAT), the Best Paper Award in the 2018 International Symposium on Antennas and Propagation (ISAP), and CAU Distinguished Scholar, from 2014 to 2020.